Article

A Comprehensive Study on Pyrolysis Mechanism of Substituted β-*O*-4 Type Lignin Dimers

Xiaoyan Jiang, Qiang Lu *, Bin Hu, Ji Liu, Changqing Dong and Yongping Yang

National Engineering Laboratory for Biomass Power Generation Equipment, North China Electric Power
University, Beijing 102206, China; jiangxiaoyan@ncepu.edu.cn (X.J.); hubin@ncepu.edu.cn (B.H.);
liujipower@ncepu.edu.cn (J.L.); dongcq@ncepu.edu.cn (C.D.); yyp@ncepu.edu.cn (Y.Y.)
* Correspondence: qlu@ncepu.edu.cn; Tel.: +86-10-6177-2030

Abstract: In order to understand the pyrolysis mechanism of β-*O*-4 type lignin dimers, a pyrolysis
model is proposed which considers the effects of functional groups (hydroxyl, hydroxymethyl and
methoxyl) on the alkyl side chain and aromatic ring. Furthermore, five specific β-*O*-4 type lignin
dimer model compounds are selected to investigate their integrated pyrolysis mechanism by density
functional theory (DFT) methods, to further understand and verify the proposed pyrolysis model.
The results indicate that a total of 11 pyrolysis mechanisms, including both concerted mechanisms
and homolytic mechanisms, might occur for the initial pyrolysis of the β-*O*-4 type lignin dimers.
Concerted mechanisms are predominant as compared with homolytic mechanisms throughout
unimolecular decomposition pathways. The competitiveness of the eleven pyrolysis mechanisms
are revealed via different model compounds, and the proposed pyrolysis model is ranked in full
consideration of functional groups effects. The proposed pyrolysis model can provide a theoretical
basis to predict the reaction pathways and products during the pyrolysis process of β-*O*-4 type
lignin dimers.

Keywords: lignin model compound; β-*O*-4 linkage; functional group; pyrolysis mechanism; density
functional theory

1. Introduction

Lignin is the most abundant renewable aromatic biopolymer in nature, biosynthesized through
polymerization of three basic monolignols, i.e., *p*-coumaryl, coniferyl, and sinapyl alcohols which
are interlinked by C–O bonds (e.g., β-*O*-4, α-*O*-4 and 4-*O*-5) and C–C bonds (e.g., β-1, β-5 and
5-5) [1–4]. Apart from different linkages, there are various functional groups on the alkyl side chain
and aromatic ring of the lignin basic units, including methoxyl, hydroxyl, hydroxymethyl, carbonyl
and more [5–7]. Among them, methoxyl, hydroxyl and hydroxymethyl groups are native substituents
while others (such as carbonyls) are non-native and chemically modified via the oxidization of the
OH group on the C_α or C_γ positions [1,6]. Therefore, lignin is the most complex component among
the three basic components of lignocellulosic biomass. Pyrolysis is a promising thermo-chemical
conversion method for the utilization of lignocellulosic biomass materials [8–10], through which
lignin can be decomposed to form various value-added aromatic compounds [9,11,12]. However,
conventional pyrolysis is a non-selective process, and it has difficulty selectively controlling the lignin
decomposition process towards specific aromatic compounds. In order to develop more efficient
selective pyrolysis techniques, lignin pyrolysis mechanism and products formation pathways should
be deeply uncovered to help provide a theoretical basis for directional control of the lignin pyrolysis
process. Density functional theory (DFT) method is an effective tool to reveal the lignin pyrolysis
mechanism at a micro level [13–16].

Due to the complex structure of natural lignin, lignin-based model compounds are widely used to investigate the pyrolysis mechanism of lignin. Considering that the β-*O*-4 linkage is dominant, accounting for about half of the linkages in lignin, β-*O*-4 type lignin dimer model compounds are typically selected for theoretical studies [13,17–19]. Previous research has investigated the pyrolysis mechanism of various β-*O*-4 type lignin dimer model compounds containing different functional groups on the alkyl side chain and aromatic ring [20,21]. Beste et al. [20] considered that phenethyl phenyl ether (PPE) mainly underwent C_β–O bond and C_α–C_β bond homolytic cleavage reactions during the primary pyrolysis process. However, Elder et al. [21] found that two concerted reactions (retro-ene fragmentation and Maccoll elimination) were prior to C_β–O bond and C_α–C_β bond homolytic cleavage reactions, and the energy barrier of retro-ene fragmentation was lower than that of Maccoll elimination. Currently, it is widely recognized that concerted reactions and homolytic reactions are coexisting during the lignin pyrolysis process [19,22]. Nevertheless, functional groups on the alkyl side chain and aromatic ring may have great effects on lignin pyrolysis mechanism. Basically, they can influence the bond dissociation energies (BDEs) of major bonds [5,6,17] and enrich the reaction pathways, including both concerted reaction pathways and homolytic reaction pathways [13,23]. Some experimental studies have also confirmed that functional groups could affect the thermal behavior and product distribution of lignin [24–27]. Kawamoto et al. [24,27] studied the effect of hydroxyl groups at C_α and C_γ positions of the alkyl side chain on pyrolytic reactions of β-*O*-4 type lignin dimer model compounds. Results suggested that the hydrogen bond between the two hydroxyl groups would affect the reaction sequences of C_γ–elimination and C_β–O bond homolytic cleavage, and further influence the product distribution. Britt et al. [28] found that the methoxyl group on the aromatic ring would weaken the C_β–O bond and make it easier to undergo homolytic reaction. Furthermore, the methoxyl group would promote O–CH_3 bond homolytic cleavage [23,29], and the hydroxyl group on the alkyl side chain would transform into ketone or accelerate the dehydration reaction [13]. However, there are few comprehensive studies focusing on the effects of these substituents on the unimolecular decomposition pathways of lignin.

Due to the limitation of previous studies, a pyrolysis model for β-*O*-4 type lignin dimers is proposed which takes the effects of native substituents (hydroxyl, hydroxymethyl and methoxyl) located on alkyl side chain and aromatic ring into consideration. The above three substituents are very common and characteristic in the natural lignin structure [6,17]. Furthermore, five specific β-*O*-4 type lignin dimer model compounds containing hydroxyl, hydroxymethyl and methoxyl groups are selected to reveal their pyrolysis mechanism by DFT calculation and to understand the proposed pyrolysis model.

2. Results

2.1. Pyrolysis Model for β-*O*-4 Type Lignin Dimers

Based on the possible pyrolysis reactions and previous studies [13,23,29], a pyrolysis model for β-*O*-4 type lignin dimers (LD) is proposed as shown in Figure 1, which considers the effects of hydroxyl, hydroxymethyl, and methoxyl groups on pyrolysis pathways. Mechanisms 1–9 are concerted reactions, while mechanisms 10 and 11 are homolytic reactions. Among them, mechanisms 1, 2 and 11 are three basic pyrolysis mechanisms for all β-*O*-4 type lignin dimers regardless of substituents. They are Maccoll elimination, retro-ene fragmentation and C_β–O bond homolytic cleavage, respectively [21].

When the methoxyl group is located on the aromatic ring of β-*O*-4 type lignin dimer model compounds, mechanisms 3 and 10 will take place. Mechanism 3 is another retro-ene fragmentation. The H atom at C_α position transfers to aromatic carbon atom where the methoxyl group is located. Mechanism 10 is O–CH_3 bond homolytic cleavage reaction. Britt et al. [29] found that O–CH_3 bond as well as C_β–O bond were the weakest bonds in lignin which were easy to break during the primary pyrolysis process.

When the hydroxyl group substitutes at C_α position, mechanisms 4, 5 and 6 will occur. Mechanism 4 is a dehydration reaction. The hydroxyl group at C_α position and the H atom at C_β position undergo dehydration reaction to form a compound containing an unsaturated C=C double bond. In mechanisms 5 and 6, the H atom of the hydroxyl group at C_α position will transfer to the oxygen atom of ether bond and C_β position meanwhile rupturing the C_β–O and C_α–C_β bonds, respectively.
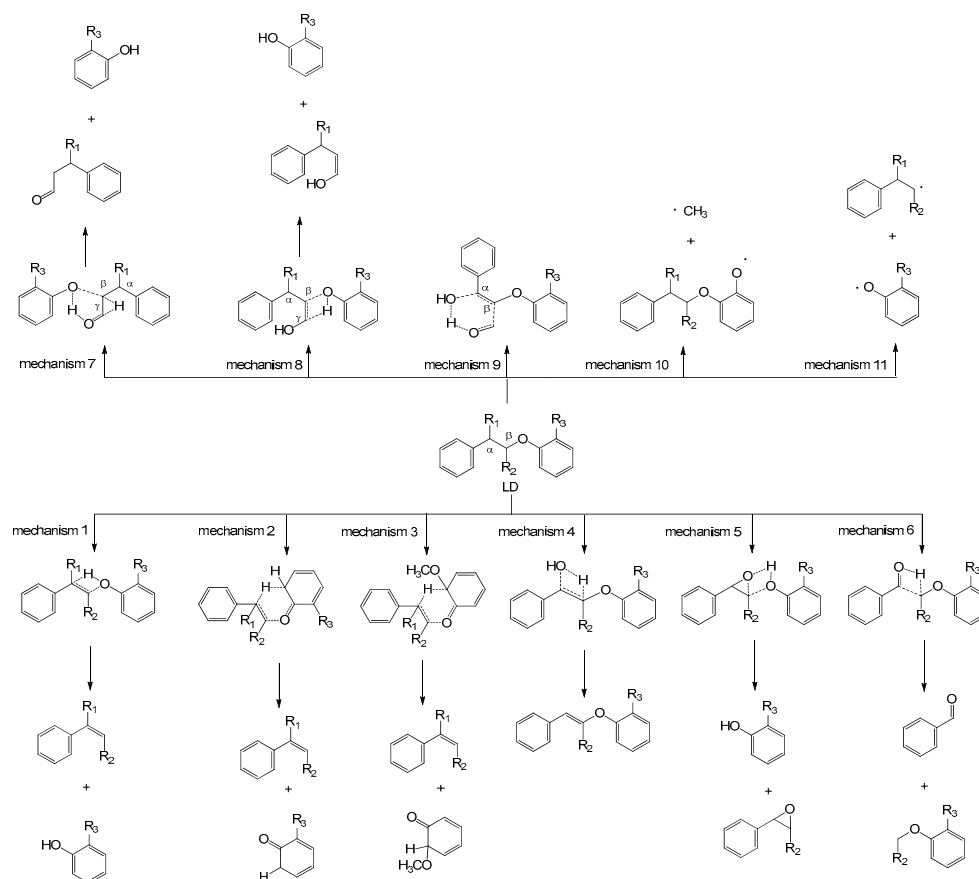
Figure 1. Pyrolysis model for β-*O*-4 type lignin dimers (LD).

When the hydroxymethyl group substitutes at C_β position, mechanisms 7 and 8 will take place through which the H atoms of hydroxyl group and C_γ position will transfer to the oxygen atom of ether bond with the rupture of C_β–O bond, respectively. When the hydroxyl and hydroxymethyl groups are located on the C_α and C_β positions of a β-*O*-4 type lignin dimer model compound, it will undergo mechanism 9 to form water, formaldehyde and a compound with an unsaturated C=C double bond.

The pyrolysis model in Figure 1 depicts possible pyrolysis pathways of β-*O*-4 type lignin dimers during the primary pyrolysis process, which just provides the basic information to predict possible pyrolytic products formed in the subsequent pyrolysis process. In the following section, five specific model compounds will be employed to investigate their detailed pyrolysis pathways based on this model, to illustrate the competitiveness of possible pyrolytic pathways.

2.2. Pyrolysis Mechanism of β-O-4 Type Lignin Dimers Based on the Pyrolysis Model

In order to further understand the proposed pyrolysis model and explore the effects of hydroxyl, hydroxymethyl and methoxyl groups on the unimolecular decomposition pathways of β-*O*-4 type lignin dimers, five specific model compounds are selected to investigate their detailed pyrolysis mechanisms and pathways, including phenethyl phenyl ether (PPE), 1-methoxy-2-phenethoxybenzene (*o*-CH₃O-PPE), 2-phenoxy-1-phenylethanol (α-OH-PPE),

2-phenoxy-3-phenylpropan-1-ol (β-CH$_2$OH-PPE), and 2-(2-methoxyphenoxy)-1-phenylpropane-1,3-diol (α-OH-β-CH$_2$OH-*o*-CH$_3$O-PPE). The detailed integrated pyrolysis mechanism of α-OH-β-CH$_2$OH-*o*-CH$_3$O-PPE is discussed below and categorized into concerted mechanisms and homolytic mechanisms. Others are shown in the Supplementary Materials (Figures S1–S4).

2.2.1. Concerted Mechanisms of Model Compound α-OH-β-CH$_2$OH-*o*-CH$_3$O-PPE

Pyrolysis of model compound α-OH-β-CH$_2$OH-*o*-CH$_3$O-PPE involves nine possible concerted mechanisms (mechanisms 1–9 in Figure 1) due to the presence of the substituents. The possible reaction pathways following the nine concerted mechanisms are designed in Figure 2 and the potential energy profile along the pathways is shown in Figure 3.
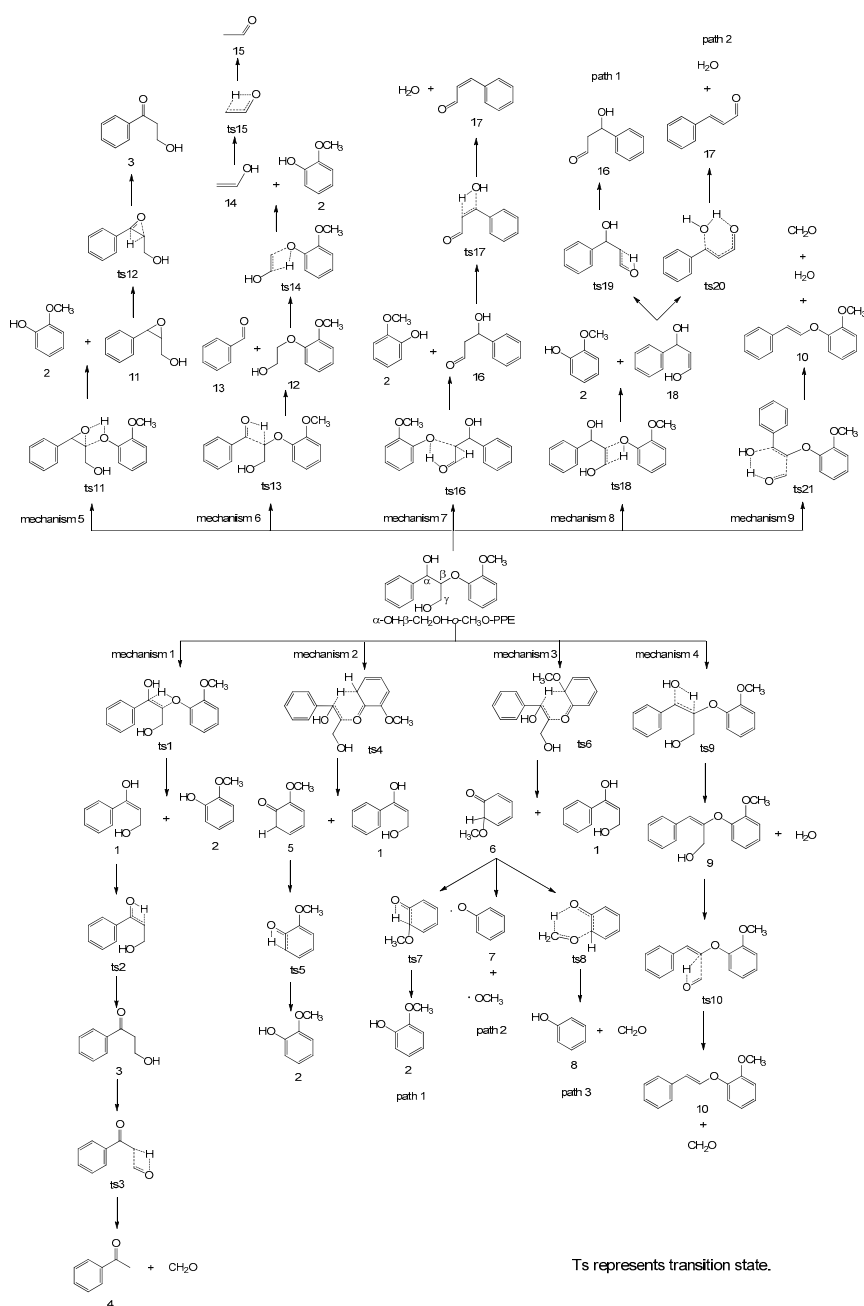
Figure 2. Possible reaction pathways based on concerted mechanisms 1–9 of the β-*O*-4 type lignin dimer model compound α-OH-β-CH$_2$OH-*o*-CH$_3$O-PPE.
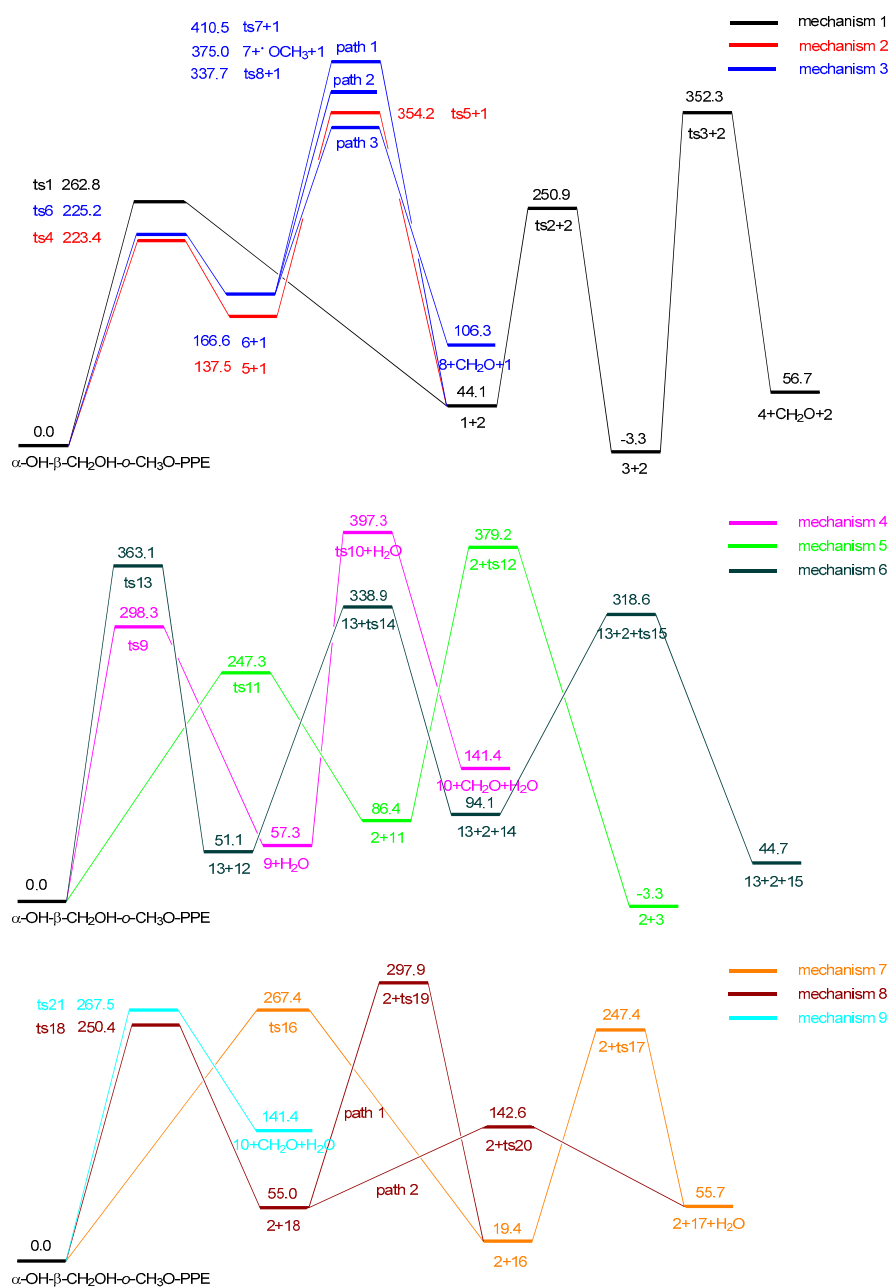
Figure 3. Potential energy profile along the reaction pathways based on concerted mechanisms 1–9.

Mechanisms 1 and 2 are the two common concerted mechanisms existing in the pyrolysis process of all β-*O*-4 type lignin dimers [21]. In concerted mechanism 1, α-OH-β-CH$_2$OH-*o*-CH$_3$O-PPE undergoes Maccoll elimination through a four-membered ring transition state **ts1** with an energy barrier of 262.8 kJ/mol. The H atom at C$_\alpha$ position transfers to the oxygen atom of the ether bond. Simultaneously, the C$_\beta$–O bond ruptures and the C$_\alpha$–C$_\beta$ bond transforms into C=C double bond, forming intermediate **1** and product **2** (2-methoxyphenol). Intermediate **1** contains an extremely unstable enol structure which easily undergoes isomerization through transition state **ts2** to generate product **3** (3-hydroxy-1-phenylpropan-1-one) with a ketone structure, overcoming an energy barrier of 206.8 kJ/mol. Product **3** with the hydroxymethyl group at C$_\beta$ position may undergo a secondary reaction via a four-membered ring transition state **ts3** to form product **4** (acetophenone) and formaldehyde, overcoming an energy barrier of 355.6 kJ/mol.

In concerted mechanism 2, α-OH-β-CH$_2$OH-*o*-CH$_3$O-PPE firstly undergoes retro-ene fragmentation through a six-membered ring transition state **ts4** to form intermediates **1** and **5** with an energy barrier of 223.4 kJ/mol, which is lower than the energy barrier of **ts1** in concerted mechanism 1. Intermediate **5** then undergoes intramolecular hydrogen transfer reaction through transition state **ts5** to form product **2** (2-methoxyphenol) with an energy barrier of 216.7 kJ/mol. Intermediate **1** will transform into product **3** (3-hydroxy-1-phenylpropan-1-one) following the reaction pathway in concerted mechanism 1.

Concerted mechanism 3 is similar to concerted mechanism 2. The only difference is that the H atom at C$_\alpha$ position transfers to the aromatic carbon atom where methoxyl group is located through transition state **ts6** with an energy barrier of 225.2 kJ/mol, forming intermediates **1** and **6**. The energy barrier of **ts6** is close to that of **ts4** in concerted mechanism 2. Intermediate **6** has three possible subsequent reaction pathways. In path 1, it undergoes intramolecular hydrogen transfer reaction through transition state **ts7** to form product **2** (2-methoxyphenol) with an energy barrier of 243.9 kJ/mol. Due to the existence of the methoxyl group, intermediate **6** can also undergo paths 2 and 3. In path 2, it undergoes demethoxylation to generate radical **7** with an energy barrier of 208.4 kJ/mol. In path 3, it undergoes intramolecular hydrogen transfer reaction through a six-membered ring transition state **ts8** to form product **8** (phenol) and formaldehyde, overcoming the lowest energy barrier of 171.1 kJ/mol. Therefore, path 3 is most likely to occur among the three possible subsequent reaction pathways in concerted mechanism 3.

Mechanisms 4–6 are closely related to the hydroxyl group at C$_\alpha$ position. In concerted mechanism 4, the hydroxyl group at C$_\alpha$ position and the H atom at C$_\beta$ position of α-OH-β-CH$_2$OH-*o*-CH$_3$O-PPE undergo dehydration reaction through a four-membered ring transition state **ts9** to form intermediate **9**, overcoming an energy barrier of 298.3 kJ/mol. Then intermediate **9** will lose a molecule of formaldehyde through transition state **ts10** to form product **10** (1-methoxy-2-(styryloxy)benzene) with an energy barrier of 340.0 kJ/mol due to the hydroxymethyl group at C$_\beta$ position.

In concerted mechanism 5, α-OH-β-CH$_2$OH-*o*-CH$_3$O-PPE goes through transition state **ts11** to form product **2** (2-methoxyphenol) and intermediate **11** with an energy barrier of 247.3 kJ/mol, through which the H atom of the hydroxyl group at C$_\alpha$ position transfers to the oxygen atom of the ether bond. Intermediate **11** then undergoes transition state **ts12** to form product **3** (3-hydroxy-1-phenylpropan-1-one) with an energy barrier of 292.8 kJ/mol.

In concerted mechanism 6, the H atom of the hydroxyl group at C$_\alpha$ position of α-OH-β-CH$_2$OH-*o*-CH$_3$O-PPE transfers to C$_\beta$ position and the C$_\alpha$–C$_\beta$ bond breaks to form intermediate **12** and product **13** (benzaldehyde) with an energy barrier of 363.1 kJ/mol. Intermediate **12** goes through a four membered ring transition state **ts14** to form product **2** (2-methoxyphenol) and intermediate **14** with an energy barrier of 287.8 kJ/mol. Intermediate **14** will undergo isomerization through transition state **ts15** to form product **15** (acetaldehyde) with an energy barrier of 224.5 kJ/mol.

Mechanisms 7 and 8 are closely related to the hydroxymethyl group at C$_\beta$ position. In concerted mechanism 7, the H atom of the hydroxyl group at C$_\gamma$ position of α-OH-β-CH$_2$OH-*o*-CH$_3$O-PPE transfers to the oxygen atom of the ether bond through transition state **ts16** to generate product **2** (2-methoxyphenol) and intermediate **16**, overcoming an energy barrier of 267.4 kJ/mol. The hydroxyl group at C$_\alpha$ position and the H atom at C$_\beta$ position of intermediate **16** undergo dehydration reaction with an energy barrier of 228.0 kJ/mol, forming product **17** (3-phenylacrylaldehyde).

In concerted mechanism 8, α-OH-β-CH$_2$OH-*o*-CH$_3$O-PPE goes through transition state **ts18** to generate product **2** (2-methoxyphenol) and intermediate **18** with an energy barrier of 250.4 kJ/mol, through which the H atom at C$_\gamma$ position transfers to the oxygen atom of the ether bond. The enol structure of intermediate **18** is easy to undergo isomerization through transition state **ts19** to form intermediate **16** with an energy barrier of 242.9 kJ/mol. Then intermediate **16** will transform into product **17** (3-phenylacrylaldehyde) following the reaction pathway in concerted mechanism 7. In addition to the isomerization reaction, intermediate **18** can also undergo dehydration reaction through a six-membered ring transition state **ts20** to form product **17** (3-phenylacrylaldehyde) with

an energy barrier of 87.6 kJ/mol, which is much lower than the energy barrier of **ts19**. Therefore, it is much easier for intermediate **18** to go through the dehydration reaction to form product **17**.

Concerted mechanism 9 is related to both the hydroxyl group at C_α position and the hydroxymethyl group at C_β position. α-OH-β-CH$_2$OH-*o*-CH$_3$O-PPE undergoes a six membered ring transition state **ts21** to directly form product **10** (1-methoxy-2-(styryloxy)benzene) with an energy barrier of 267.5 kJ/mol, losing a molecule of water and formaldehyde.

According to the above results, the sequence of energy barriers of the above nine concerted mechanisms is as follows: mechanism 2 < mechanism 3 < mechanism 5 < mechanism 8 < mechanism 1 < mechanism 7 < mechanism 9 < mechanism 4 < mechanism 6. The primary aromatic products are **2** (2-methoxyphenol), **3** (3-hydroxy-1-phenylpropan-1-one), **8** (phenol), **17** (3-phenylacrylaldehyde), **10** (1-methoxy-2-(styryloxy)benzene) and **13** (benzaldehyde), as well as some low molecular compounds (formaldehyde, water and acetaldehyde). As shown in Figure 3, these products are formed via different mechanisms. Products **2** and **3** can be formed from mechanisms 1, 2 and 5, among which the energy barrier of mechanism 2 is the lowest. Mechanism 8 is superior to mechanism 7 to form product **17**, and mechanism 9 is superior to mechanism 4 to form product **10**. In regard to products **8** and **13**, their formation pathways are attributed to mechanisms 3 and 6, respectively.

2.2.2. Homolytic Mechanisms of Model Compound α-OH-β-CH$_2$OH-*o*-CH$_3$O-PPE

The possible homolytic cleavage reactions of the major bonds and their corresponding BDEs are illustrated in Figure 4. Compared with other homolytic cleavage reactions, the O–CH$_3$ bond homolytic cleavage (mechanism 10) has the lowest BDE, followed by the C_β–O bond homolytic cleavage (mechanism 11), indicating that mechanisms 10 and 11 are the two favorable homolytic mechanisms of lignin model compound α-OH-β-CH$_2$OH-*o*-CH$_3$O-PPE. Other homolytic cleavage reactions can hardly take place due to the high BDEs. Such results also reflect that the proposed pyrolysis model in Figure 1 is reasonable. Except for concerted mechanisms 4 and 6, the activation energies of other concerted mechanisms are lower than the BDEs of homolytic mechanisms during the primary pyrolysis process. Hence, it can be concluded that concerted mechanisms should be mainly responsible for the pyrolysis process, while homolytic mechanisms are less important than concerted mechanisms. The subsequent pyrolysis pathways based on mechanisms 10 and 11 are discussed below.
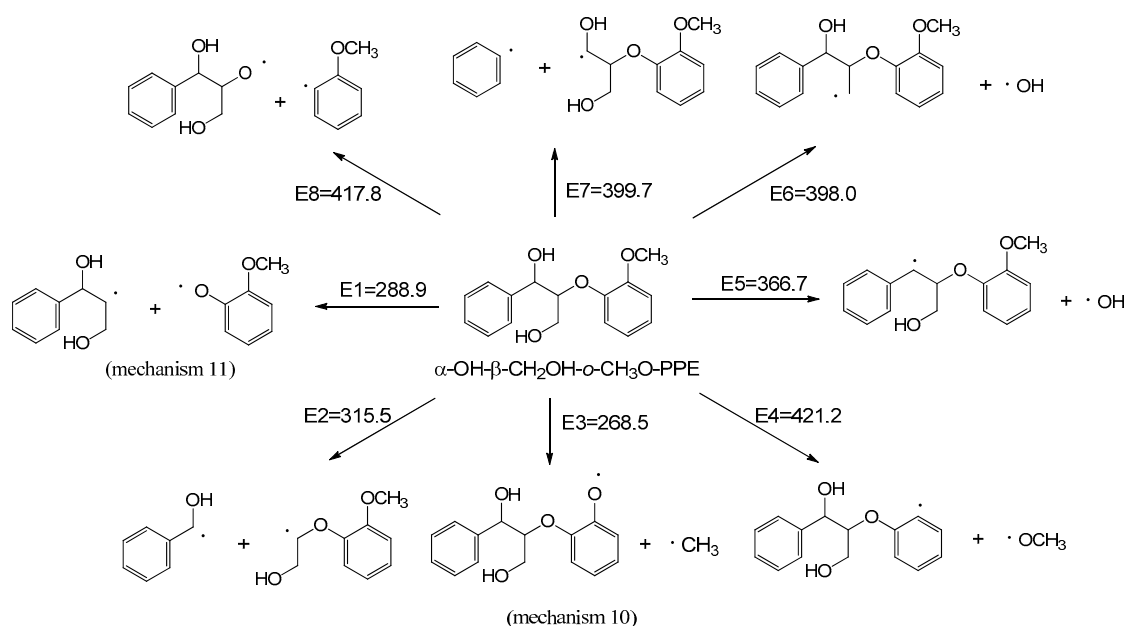

Figure 4. Bond dissociation energies of the major bonds in lignin model compound α-OH-β-CH$_2$OH-*o*-CH$_3$O-PPE (unit: kJ/mol).

In homolytic mechanism 10, α-OH-β-CH$_2$OH-o-CH$_3$O-PPE undergoes O–CH$_3$ bond homolytic cleavage to form radical **19** and methyl radical with an energy barrier of 268.5 kJ/mol. As shown in Figure 5, radical **19** has four possible subsequent reaction pathways. The potential energy profile along reaction pathways for the homolytic cleavage of O–CH$_3$ bond is shown in Figure 6.
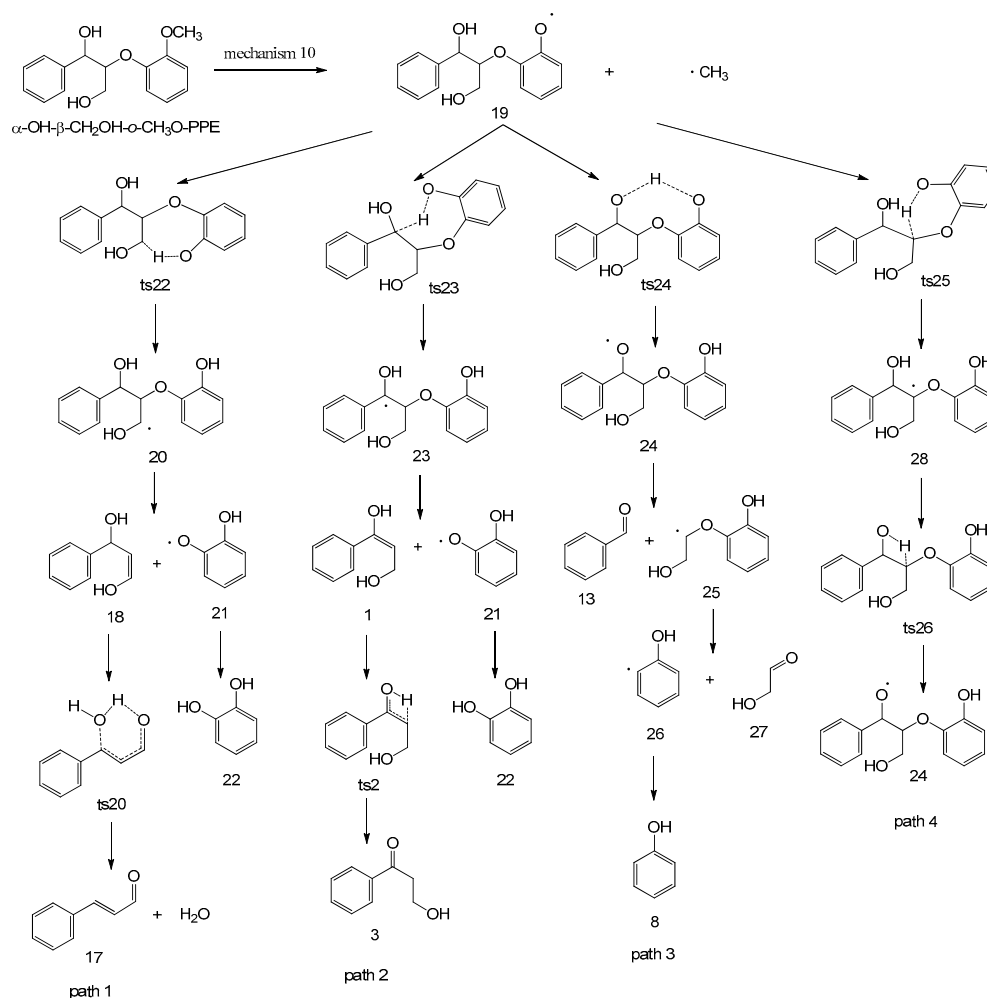
Figure 5. Possible reaction pathways based on O–CH$_3$ bond homolytic cleavage of α-OH-β-CH$_2$OH-o-CH$_3$O-PPE.
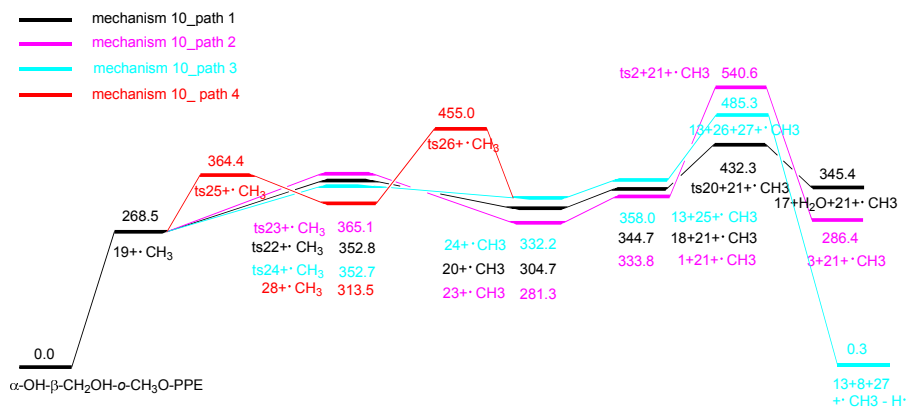
Figure 6. Potential energy profile along reaction pathways for the homolytic cleavage of O–CH$_3$ bond.

In path 1, the H atom at C_γ position of radical **19** transfers to phenoxy radical through a seven-membered ring transition state **ts22** to form radical **20** with an energy barrier of 84.3 kJ/mol. Radical **20** undergoes further C_β–O bond homolytic cleavage to form intermediate **18** and radical **21** with an energy barrier of 40.0 kJ/mol. Radical **21** will couple with free H radical to form hydrogenated product **22** (catechol). Intermediate **18** will transform into product **17** (3-phenylacrylaldehyde) following the reaction pathway in concerted mechanism 8.

In path 2, the H atom at C_α position of radical **19** transfers to phenoxy radical through a seven-membered ring transition state **ts23** to form radical **23** with an energy barrier of 96.6 kJ/mol. Radical **23** further undergoes C_β–O bond homolytic cleavage to generate intermediate **1** and radical **21** with an energy barrier of 52.5 kJ/mol. Intermediate **1** will transform into product **3** (3-hydroxy-1-phenylpropan-1-one) following the reaction pathway in concerted mechanism 1.

In path 3, the H atom of the hydroxyl group at C_α position of radical **19** transfers to phenoxy radical through an eight-membered ring transition state **ts24** to form radical **24** with an energy barrier of 84.2 kJ/mol. Then radical **24** undergoes C_α–C_β bond homolytic cleavage to form product **13** (benzaldehyde) and radical **25** with an energy barrier of 25.8 kJ/mol. Radical **25** continues to undergo $C_{aromatic}$–O bond homolytic cleavage to form radical **26** and product **27** (hydroxyacetaldehyde) with an energy barrier of 127.3 kJ/mol. Radical **26** will combine with free H radical to form hydrogenated product **8** (phenol).

In path 4, radical **19** undergoes intramolecular hydrogen transfer reactions through two consecutive transition states **ts25** and **ts26** to form radical **24** with energy barriers of 95.9 kJ/mol and 141.5 kJ/mol, respectively. Radical **24** will follow path 3 to undergo subsequent reactions. Comparing the energy barriers to form radical **24** in paths 3 and 4, path 3 is superior to path 4 due to its lower energy barrier.

The above four subsequent pyrolysis pathways based on homolytic mechanism 10 are competitive with each other. As shown in Figure 6, the energy barriers of **ts22** and **ts24** are close and lower than those of **ts23** and **ts25**. Hence, the major pyrolytic products based on mechanism 10 include **17** (3-phenylacrylaldehyde), **22** (catechol), **13** (benzaldehyde), **8** (phenol) and **27** (hydroxyacetaldehyde). Products **17** and **13** can also be formed through concerted mechanisms 8 and 6, respectively. In comparison of concerted mechanism 8 and homolytic mechanism 10, product **17** is easily formed from concerted mechanism 8, while product **13** is easily formed from homolytic mechanism 10.

In homolytic mechanism 11, α-OH-β-CH_2OH-*o*-CH_3O-PPE undergoes C_β–O bond homolytic cleavage to form radicals **29** and **30** with an energy barrier of 288.9 kJ/mol. The subsequent pyrolysis pathways of radicals **29** and **30** are shown in Figure 7, and the corresponding potential energy profile is depicted in Figure 8. Radical **29** has four possible following pathways. It loses the hydroxyl groups at C_γ and C_α positions to form products **31** (1-phenylprop-2-en-1-ol) and **32** (3-phenylprop-2-en-1-ol) with energy barriers of 130.0 kJ/mol and 123.2 kJ/mol, respectively. Or it undergoes dehydrogenation reactions at C_α and C_γ positions to form intermediates **1** and **18** with energy barriers of 130.5 kJ/mol and 141.5 kJ/mol, respectively. They will follow the reaction pathways in concerted mechanisms 1 and 8 to form products **3** (3-hydroxy-1-phenylpropan-1-one) and **17** (3-phenylacrylaldehyde). As shown in Figure 8, the above four pathways of radical **29** are competitive with each other, among which path 2 has the lowest energy barrier to form product **32** (3-phenylprop-2-en-1-ol).

Radical **30** can undergo a series of reactions to form product **36** (2-hydroxybenzaldehyde). It firstly undergoes intramolecular hydrogen transfer reaction through a six-membered ring transition state **ts27** to form radical **33** with an energy barrier of 102.9 kJ/mol. Radical **33** then goes through C–O shift reaction via two consecutive transition states **ts28** and **ts29** to form radical **35** with energy barriers of 73.2 kJ/mol and 7.2 kJ/mol, respectively. Radical **35** finally undergoes dehydrogenation reaction to form product **36** (2-hydroxybenzaldehyde) with an energy barrier of 52.6 kJ/mol. Hence, the major pyrolytic products based on homolytic mechanism 11 (paths 2 and 5) are **32** (3-phenylprop-2-en-1-ol) and **36** (2-hydroxybenzaldehyde).
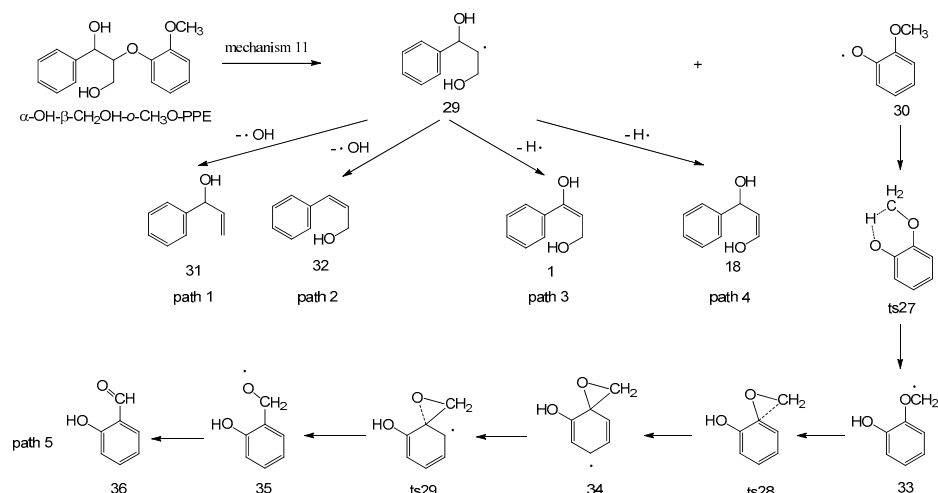
Figure 7. Possible reaction pathways based on C_β–O bond homolytic cleavage of α-OH-β-CH$_2$OH-o-CH$_3$O-PPE.
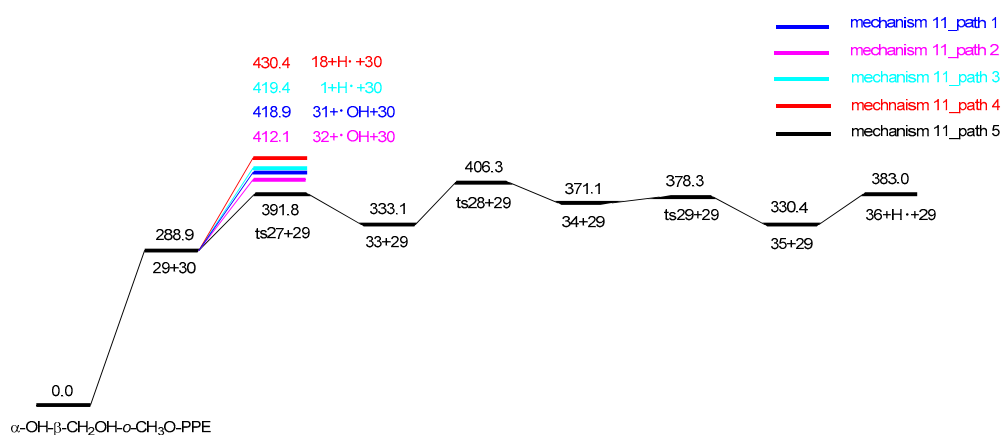
Figure 8. Potential energy profile along reaction pathways for the homolytic cleavage of C_β–O bond (unit: kJ/mol).

2.2.3. Summary

Based on the energy barriers of the above 11 pyrolysis mechanisms of α-OH-β-CH$_2$OH-o-CH$_3$O-PPE, their competitiveness will follow this order, i.e., mechanism 2 > mechanism 3 > mechanism 5 > mechanism 8 > mechanism 1 > mechanism 7 > mechanism 9 > mechanism 10 > mechanism 11 > mechanism 4 > mechanism 6. Among the unimolecular decomposition pathways of α-OH-β-CH$_2$OH-o-CH$_3$O-PPE, most of the concerted mechanisms are superior to homolytic mechanisms except for mechanism 6. The major pyrolytic products based on concerted mechanisms include **2** (2-methoxyphenol), **3** (3-hydroxy-1-phenylpropan-1-one), **8** (phenol), **10** (1-methoxy-2-(styryloxy)benzene) and **17** (3-phenylacrylaldehyde). While the pyrolytic products based on O–CH$_3$ and C_β–O bond homolytic mechanisms include **13** (benzaldehyde), **22** (catechol), **32** (3-phenylprop-2-en-1-ol) and **36** (2-hydroxybenzaldehyde). Product **2** (2-methoxyphenol) is the most abundant product generated from most of the concerted mechanisms with relatively low energy barriers. In addition, radical **30** formed from C_β–O bond homolytic mechanism can also combine with free H radical and undergo H-abstraction to form product **2** (2-methoxyphenol) [20,23,30]. It agrees with the results obtained by He et al. [22] and Jiang et al. [31]. They conducted pyrolysis experiments on a β-O-4 type lignin dimer model compound (guaiacylglycerol-β-guaiacyl ether) which has same functional groups on the alkyl side chain and aromatic ring near the ether bond.

They found that 2-methoxyphenol was the major product while the other products were in low yields. These experimental results firmly confirm that the proposed pyrolysis model in Figure 1 is reasonable and reliable.

The integrated pyrolysis mechanisms of the other four β-*O*-4 type lignin model compounds PPE, α-OH-PPE, β-CH$_2$OH-PPE and *o*-CH$_3$O-PPE are depicted in the Supplementary Materials (Figures S1–S4) based on the proposed pyrolysis model in Figure 1. Pyrolysis of PPE may follow mechanisms 1, 2 and 11 to decompose, and their competitiveness is in the order of mechanism 2 > mechanism 1 > mechanism 11. α-OH-PPE may undergo pyrolysis reactions through mechanisms 1, 2, 4, 5, 6 and 11, and their competitiveness follows the order of mechanism 2 > mechanism 1 > mechanism 4 > mechanism 11 > mechanism 5 > mechanism 6. β-CH$_2$OH-PPE may follow five pyrolysis mechanisms to decompose, whose competitiveness order is mechanism 2 > mechanism 1 > mechanism 7 > mechanism 8 > mechanism 11. *o*-CH$_3$O-PPE also has five possible pyrolysis mehanisms with the competitiveness order of mechanism 2 > mechanism 3 > mechanism 1 > mechanism 10 > mechanism 11. It is important to note that the major pyrolytic products of the four model compounds obtained through DFT calculations shown in the Supplementary Materials agree well with the experimental results [18,19,29,31], which futher confirms the validity of the pyrolysis model. Based on the results, a similar conclusion can be drawn that most of the concerted mechanisms are prior to homolytic mechanisms, except for mechanism 6. The above results clearly illustrate that based on the pyrolysis model proposed in Figure 1, the pyrolysis mechanisms for different β-*O*-4 type lignin dimer model compounds basically follow certain specific rules, but different functional groups will affect the pyrolytic product distribution. Hence, the pyrolysis model in Figure 1 can be used to predict the pyrolytic pathways and products.

3. Discussion

According to the above analyses, concerted mechanisms and homolytic mechanisms are coexisting in the pyrolysis process of β-*O*-4 type lignin dimer model compounds. Moreover, concerted mechanisms are generally prior to homolytic mechanisms, indicating concerted mechanisms are dominant for the pyrolysis process. Mechanisms 1, 2 and 11 are fundamental for all β-*O*-4 type lignin dimer model compounds and their competitiveness follows the order of mechanism 2 > mechanism 1 > mechanism 11, which is irrelevant to the hydroxyl, hydroxymethyl and methoxyl groups. In consideration of the effects of functional groups, the competitiveness of the proposed 11 pyrolysis mechanisms for different β-*O*-4 type lignin dimers can be concluded in the order of mechanism 2 > mechanism 3 > mechanism 1 > mechanism 7 > mechanism 9 > mechanism 10 > mechanism 11 > mechanism 6, wherein mechanisms 4, 5 and 8 can hardly be ranked because their competitiveness is dramatically affected by the functional groups on the aromatic ring and alkyl side chain. Among these mechanisms, mechanism 3 is quite competitive with mechanism 2 (retro-ene fragmentation) which is considered as the dominant pyrolysis mechanism of substituted β-*O*-4 model compounds [21,23]. Mechanism 10 (O–CH$_3$ bond homolytic cleavage) will supersede mechanism 11 (C$_\beta$–O bond homolytic cleavage) to be the optimal homolytic mechanism. Mechanism 6 can hardly take place due to its high energy barrier.

The application of the proposed pyrolysis model ultimately offers a theoretical basis to predict the pyrolytic pathways and the formed products. PPE is the simplest β-*O*-4 type lignin dimer model compound [32], and the major pyrolytic products are styrene and phenol, which has been confirmed in this study as well as previous studies [29,33,34]. In the presence of functional groups on the alkyl side chain and aromatic ring, the pyrolytic product distribution will be changed, but have regularity. Pyrolysis of the methoxyl-substituted PPEs mainly proceeds through concerted mechanisms (mechanisms 1, 2, 5, 7 and 8) to produce 2-methoxyphenol (or 2,6-dimethoxyphenol) as one of the dominant pyrolytic products. Furthermore, another dominant product 2-hydroxybenzaldehyde (or 2-hydroxy-3-methoxybenzaldehyde) can be formed from a key intermediate methoxyphenoxy (or 2,6-dimethoxyphenoxy) radical through a series of reaction steps [2,29] shown in Figure 7 (mechanism 11). The α-hydroxyl-substituted PPEs may undergo dehydration reactions to form the

compounds containing an unsaturated C=C double bond through mechanisms 4. These compounds are easy to transform into macromolecular compounds and coke through polymerization [35], which may be one of the possible reasons for high char yield during lignin pyrolysis process. In addition, the major pyrolytic products from pyrolysis of α-hydroxyl-substituted PPEs have a C=O feature structure at C_α position. Similarly, the major pyrolytic products formed from pyrolysis of β-hydroxymethyl-substituted PPEs also have a C=O feature structure at C_γ position. In the following studies, the pyrolysis models for other lignin structures containing oxidized substituents and α-*O*-4, 4-*O*-5, β-1, β-5 or 5-5 linkages will be investigated to comprehensively understand the lignin pyrolysis process, which can provide theoretical guidance for developing efficient selective pyrolysis techniques.

4. Calculation Methods

All calculations were conducted in Gaussian 09 suite of programs [36]. The geometries of reactants, intermediates, transition states and products were optimized by using hybrid density functional M06-2X and the 6−31+G(d,p) basis set, followed by frequency calculations. To simulate the real pyrolysis condition, the thermodynamic parameters at typical pyrolysis temperature and pressure (873 K and 101 kPa) were obtained by frequency analyses. The transition states were located by TS method in which only the initial guesses of the transition states were used without using the corresponding initial guesses of reactants and products. Furthermore, intrinsic reaction coordinate (IRC) calculations were conducted to confirm the corresponding reactants, transition states and products on the same potential energy surface (PES). The reactants, intermediates and products had no imaginary frequency, while the transition states had only one imaginary frequency. Activation energies for concerted reactions were estimated with the energy differences between transition states and reactants. While for homolytic cleavage reactions, transition states were very difficult to find because there were no saddle points on the PES, the BDE was generally regarded as approximation to activation energy for comparison [13,34,37].

5. Conclusions

A pyrolysis model containing 11 initial pyrolysis mechanisms (mechanisms 1–11) for β-*O*-4 type lignin dimers is proposed which comprehensively considers the effects of functional groups (hydroxyl, hydroxymethyl and methoxyl) on the alkyl side chain and aromatic ring. Based on the pyrolysis model, the integrated pyrolysis mechanisms of five specific β-O-4 type lignin dimer model compounds are investigated by DFT calculations. The results indicate that among the unimolecular decomposition pathways, concerted mechanisms and homolytic mechanisms are coexisting, while concerted mechanisms are predominant and mainly responsible for the pyrolysis process. Mechanisms 1, 2 and 11 are three basic mechanisms of all β-*O*-4 type lignin dimers and their competitiveness order remains invariable (mechanism 2 > mechanism 1 > mechanism 11) regardless of functional groups. The competitiveness of the proposed 11 pyrolysis mechanisms follows the order of mechanism 2 > mechanism 3 > mechanism 1 > mechanism 7 > mechanism 9 > mechanism 10 > mechanism 11 > mechanism 6, wherein mechanisms 4, 5 and 8 can hardly be ranked in view of the effects of functional groups. Combining previous experimental studies, it can be concluded that the proposed pyrolysis model is reasonable and reliable.

Author Contributions: Xiaoyan Jiang and Qiang Lu conducted the density functional theory (DFT) calculations, data analysis and writing. Bin Hu and Ji Liu assisted with data analysis. Changqing Dong, Yongping Yang and the above authors reviewed, contributed to the revising, and agreed to the article's content.

Conflicts of Interest: The authors declare no conflict of interest.

References

1. Zakzeski, J.; Bruijnincx, P.C.A.; Jongerius, A.L.; Weckhuysen, B.M. The catalytic valorization of lignin for the production of renewable chemicals. *Chem. Rev.* **2010**, *110*, 3552–3599. [CrossRef] [PubMed]

2. Kawamoto, H. Lignin pyrolysis reactions. *J. Wood Sci.* **2017**, *63*, 117–132. [CrossRef]

3. Mu, W.; Ben, H.; Ragauskas, A.; Deng, Y. Lignin pyrolysis components and upgrading—Technology review. *Bioenergy Res.* **2013**, *6*, 1183–1204. [CrossRef]

4. Azadi, P.; Inderwildi, O.R.; Farnood, R.; King, D.A. Liquid fuels, hydrogen and chemicals from lignin: A critical review. *Renew. Sustain. Energy Rev.* **2013**, *21*, 506–523. [CrossRef]

5. Parthasarathi, R.; Romero, R.A.; Redondo, A.; Gnanakaran, S. Theoretical study of the remarkably diverse linkages in lignin. *J. Phys. Chem. Lett.* **2011**, *2*, 2660–2666. [CrossRef]

6. Kim, S.; Chmely, S.C.; Nimlos, M.R.; Bomble, Y.J.; Foust, T.D.; Paton, R.S.; Beckham, G.T. Computational study of bond dissociation enthalpies for a large range of native and modified lignins. *J. Phys. Chem. Lett.* **2011**, *2*, 2846–2852. [CrossRef]

7. Asatryan, R.; Bennadji, H.; Bozzelli, J.W.; Ruckenstein, E.; Khachatryan, L. Molecular products and fundamentally based reaction pathways in the gas-phase pyrolysis of the lignin model compound *p*-coumaryl alcohol. *J. Phys. Chem. A* **2017**, *121*, 3352–3371. [CrossRef] [PubMed]

8. Sharma, A.; Pareek, V.; Zhang, D. Biomass pyrolysis—A review of modelling, process parameters and catalytic studies. *Renew. Sustain. Energy Rev.* **2015**, *50*, 1081–1096. [CrossRef]

9. Bridgwater, A.V. Review of fast pyrolysis of biomass and product upgrading. *Biomass Bioenergy* **2012**, *38*, 68–94. [CrossRef]

10. Collard, F.X.; Blin, J. A review on pyrolysis of biomass constituents: Mechanisms and composition of the products obtained from the conversion of cellulose, hemicelluloses and lignin. *Renew. Sustain. Energy Rev.* **2014**, *38*, 594–608. [CrossRef]

11. Amen-Chen, C.; Pakdel, H.; Roy, C. Production of monomeric phenols by thermochemical conversion of biomass: A review. *Bioresour. Technol.* **2001**, *79*, 277–299. [CrossRef]

12. Wang, Q.; Guan, S.; Shen, D. Experimental and kinetic study on lignin depolymerization in water/formic acid system. *Int. J. Mol. Sci.* **2017**, *18*, 2082. [CrossRef] [PubMed]

13. Huang, J.; Liu, C.; Wu, D.; Tong, H.; Ren, L. Density functional theory studies on pyrolysis mechanism of β-*O*-4 type lignin dimer model compound. *J. Anal. Appl. Pyrolysis* **2014**, *109*, 98–108. [CrossRef]

14. Jiang, X.Y.; Lu, Q.; Ye, X.N.; Hu, B.; Dong, C.Q. Experimental and theoretical studies on the pyrolysis mechanism of β-1-type lignin dimer model compound. *BioResources* **2016**, *11*, 6232–6243. [CrossRef]

15. Wang, S.; Ru, B.; Dai, G.; Shi, Z.; Zhou, J.; Luo, Z.; Ni, M.; Cen, K. Mechanism study on the pyrolysis of a synthetic β-*O*-4 dimer as lignin model compound. *Proc. Combust. Inst.* **2017**, *36*, 2225–2233. [CrossRef]

16. Liu, C.; Wilson, A.K. Cleavage of the β-*O*-4 linkage of lignin using group 8 pincer complexes: A DFT study. *J. Mol. Catal. A Chem.* **2015**, *399*, 33–41. [CrossRef]

17. Younker, J.M.; Beste, A.; Buchanan, A.C. Computational study of bond dissociation enthalpies for substituted β-*O*-4 lignin model compounds. *ChemPhysChem* **2011**, *12*, 3556–3565. [CrossRef] [PubMed]

18. Zhang, J.J.; Jiang, X.Y.; Ye, X.N.; Chen, L.; Lu, Q.; Wang, X.H.; Dong, C.Q. Pyrolysis mechanism of a β-*O*-4 type lignin dimer model compound. *J. Therm. Anal. Calorim.* **2016**, *123*, 501–510. [CrossRef]

19. Chen, L.; Ye, X.; Luo, F.; Shao, J.; Lu, Q.; Fang, Y.; Wang, X.; Chen, H. Pyrolysis mechanism of β-*O*-4 type lignin model dimer. *J. Anal. Appl. Pyrolysis* **2015**, *115*, 103–111. [CrossRef]

20. Beste, A.; Buchanan, A.C., III. Substituent effects on the reaction rates of hydrogen abstraction in the pyrolysis of phenethyl phenyl ethers. *Energy Fuels* **2010**, *24*, 2857–2867. [CrossRef]

21. Elder, T.; Beste, A. Density functional theory study of the concerted pyrolysis mechanism for lignin models. *Energy Fuels* **2014**, *28*, 5229–5235. [CrossRef]

22. He, T.; Zhang, Y.; Zhu, Y.; Wen, W.; Pan, Y.; Wu, J.; Wu, J. Pyrolysis mechanism study of lignin model compounds by synchrotron vacuum ultraviolet photoionization mass spectrometry. *Energy Fuels* **2016**, *30*, 2204–2208. [CrossRef]

23. Wang, M.; Liu, C. Theoretic studies on decomposition mechanism of *o*-methoxy phenethyl phenyl ether: Primary and secondary reactions. *J. Anal. Appl. Pyrolysis* **2016**, *117*, 325–333. [CrossRef]

24. Kawamoto, H.; Horigoshi, S.; Saka, S. Effects of side-chain hydroxyl groups on pyrolytic β-ether cleavage of phenolic lignin model dimer. *J. Wood Sci.* **2007**, *53*, 268–271. [CrossRef]

25. Kawamoto, H.; Nakamura, T.; Saka, S. Pyrolytic cleavage mechanisms of lignin-ether linkages: A study on p-substituted dimers and trimers. *Holzforschung* **2008**, *62*, 50–56. [CrossRef]

26. Kawamoto, H.; Ryoritani, M.; Saka, S. Different pyrolytic cleavage mechanisms of β-ether bond depending on the side-chain structure of lignin dimers. *J. Anal. Appl. Pyrolysis* **2008**, *81*, 88–94. [CrossRef]

27. Kawamoto, H.; Saka, S. Role of side-chain hydroxyl groups in pyrolytic reaction of phenolic β-ether type of lignin dimer. *J. Wood Chem. Technol.* **2007**, *27*, 113–120. [CrossRef]

28. Britt, P.F.; Kidder, M.K.; Buchanan, A.C., III. Oxygen substituent effects in the pyrolysis of phenethyl phenyl ethers. *Energy Fuels* **2007**, *21*, 3102–3108. [CrossRef]

29. Britt, P.F.; Buchanan, A.C.; Cooney, M.J.; Martineau, D.R. Flash vacuum pyrolysis of methoxy-substituted lignin model compounds. *J. Org. Chem.* **2000**, *65*, 1376–1389. [CrossRef] [PubMed]

30. Elder, T. A computational study of pyrolysis reactions of lignin model compounds. *Holzforschung* **2010**, *64*, 435–440. [CrossRef]

31. Jiang, W.; Wu, S.; Lucia, L.A.; Chu, J. A comparison of the pyrolysis behavior of selected β-*O*-4 type lignin model compounds. *J. Anal. Appl. Pyrolysis* **2017**, *125*, 185–192. [CrossRef]

32. Beste, A.; Buchanan, A.C., III. Kinetic simulation of the thermal degradation of phenethyl phenyl ether, a model compound for the β-*O*-4 linkage in lignin. *Chem. Phys. Lett.* **2012**, *550*, 19–24. [CrossRef]

33. Huang, X.; Liu, C.; Huang, J.; Li, H. Theory studies on pyrolysis mechanism of phenethyl phenyl ether. *Comput. Theor. Chem.* **2011**, *976*, 51–59. [CrossRef]

34. Jarvis, M.W.; Daily, J.W.; Carstensen, H.H.; Dean, A.M.; Sharma, S.; Dayton, D.C.; Robichaud, D.J.; Nimlos, M.R. Direct detection of products from the pyrolysis of 2-phenethyl phenyl ether. *J. Phys. Chem. A* **2011**, *115*, 428–438. [CrossRef] [PubMed]

35. Nakamura, T.; Kawamoto, H.; Saka, S. Condensation reactions of some lignin related compounds at relatively low pyrolysis temperature. *J. Wood Chem. Technol.* **2007**, *27*, 121–133. [CrossRef]

36. Frisch, M.J.; Trucks, G.W.; Schlegel, H.B.; Scuseria, G.E.; Robb, M.A.; Cheeseman, J.R.; Scalmani, G.; Barone, V.; Mennucci, B.; Petersson, G.A.; et al. *Gaussian 09*; Revision D.01; Gaussian, Inc.: Wallingford, CT, USA, 2013.

37. Huang, J.; He, C. Pyrolysis mechanism of α-*O*-4 linkage lignin dimer: A theoretical study. *J. Anal. Appl. Pyrolysis* **2015**, *113*, 655–664. [CrossRef]